REPORT NO.
UCB/SEMM-96/03

STRUCTURAL ENGINEERING
MECHANICS AND MATERIALS

A MODAL ANALYSIS OF FINITE DEFORMATION ENHANCED STRAIN FINITE ELEMENTS

BY

F. ARMERO

FEBRUARY 1996

DEPARTMENT OF CIVIL AND
ENVIRONMENTAL ENGINEERING
UNIVERSITY OF CALIFORNIA
BERKELEY, CALIFORNIA

A Modal Analysis of Finite Deformation Enhanced Strain Finite Elements

by

F. ARMERO
Structural Engineering, Mechanics and Materials,
Department of Civil Engineering,
University of California at Berkeley,
Berkeley CA, 94720

Abstract

This report presents closed-form expressions for the eigenvalues and eigenvectors of enhanced strain finite elements in finite strain conditions. An undistorted square element under uniaxial tension/compression is considered in the calculations. The material model is given by a general compressible Ogden hyperelastic model. Different element enhancements are tested. The results presented herein confirm the existence of zero energy modes in compression in the original enhanced formulation of SIMO & ARMERO [1992], and indicates the absence of these modes in the new formulations presented in GLASER & ARMERO [1995]. It is further shown that models exhibiting negative axial stiffness in tension lead to negative stiffness of the transversal hourglass mode.

1. Introduction

The formulation of enhanced strain finite element methods for finite deformation methods has been considered in SIMO & ARMERO [1992], SIMO, ARMERO & TAYLOR [1993], and GLASER & ARMERO [1995], as a generalization of the infinitesimal enhanced strain elements of SIMO & RIFAI [1990]. Alternative enhancement strategies have been presented by other authors; see e.g. NAGTEGAAL & FOX [1995] and CRISFIELD et al. [1995], among others. The original strategy involves an additive enhancement of the deformation gradient resulting of the standard isoparametric bilinear interpolation. This approach leads to elements exhibiting a locking-free response in bending and the incompressible limit, maintaining a strain driven structure of the final formulation. This last property makes this formulation especially suited for the numerical implementation of general inelastic models. However, it was observed in the first of these references that the proposed element suffered of zero energy modes, which lead to severe hourglassing in compression. Modifications were presented in the following references to alleviate this problem.

The appearance of the zero energy mode in compression has been characterized analytically in WRIGGERS & REESE [1994], who calculated explicitly the eigenvalues for an undistorted element with the original enhanced formulation in plane strain conditions under uniaxial compression. The material model considered by the authors correspond to a Neo-Hookean material. We consider the same problem in this report but with a general Ogden model and involving alternative enhancements of the deformation gradient. In addition, we give closed-form expressions of the complete set of eigenvalues and eigenvectors of the element, thus allowing the understanding of the response of the elements under consideration.

The rest of this report is organized as follows. Section 2 includes a summary of the formulation of enhanced strain finite element methods. The characterization of the elastic material model consider herein is presented in Section 2.2.1. Section 3 presents the calculations leading to the closed-form expressions of the eigenpairs of the finite elements under consideration. A discussion of the results is presented in Section 4, for different particular material models. Finally, Section 5 presents some concluding remarks.

2. The Enhanced Strain Finite Element Method

This section presents a summary of the general formulation of enhanced strain finite element methods in finite deformation problems. The reader is referred to the original references SIMO & ARMERO [1992], SIMO, ARMERO & TAYLOR [1993], and GLASER & ARMERO [1995], for complete details.

2.1. The Enhanced Deformation Gradient

Denote by Ω^h a discretization in quadrilateral finite elements of a domain $\Omega \subset \mathbb{R}^2$ occupied by the reference placement of a solid $\mathcal{B}$. Let $\boldsymbol{\varphi}^h : \Omega^h \to \mathbb{R}^2$ be a piecewise bilinear isoparametric interpolation of the deformation $\boldsymbol{\varphi}(\boldsymbol{X})$ for $\boldsymbol{X} \in \Omega$, that is, at the element Ω_e^h we have

$$\boldsymbol{\varphi}_e^h(\boldsymbol{X}) = \sum_{A=1}^{n_{\text{node}}} (\boldsymbol{X}_A + \boldsymbol{d}_A) N^A \circ \hat{\boldsymbol{X}}^{-1} , \tag{2.1}$$

where $\boldsymbol{X} = \hat{\boldsymbol{X}}(\boldsymbol{\xi})$ denotes the isoparametric map $\hat{\boldsymbol{X}} : \square \to \Omega_e^h$ from the parent domain $\square := [-1, 1]^2$. Here, the vectors $\boldsymbol{d}_A \in \mathbb{R}^2$ denote the unknown 4 nodal displacements, $\boldsymbol{X}_A \in \mathbb{R}^{n_{\text{dim}}}$ are the nodal reference coordinates, and N^A are the standard isoparametric shape functions, that is,

$$N^A(\boldsymbol{\xi}) := \frac{1}{4}(1 + \xi^A \xi)(1 + \eta^A \eta) , \quad \text{for } \boldsymbol{\xi} = (\xi, \eta) \in \square , \tag{2.2}$$

in 2D, where (ξ^A, η^A) for $A = 1, 4$ are the vertices of the parent domain $\square$. Similar constructions apply to 3D problems.

Our point of departure is the three-step procedure described in SIMO, ARMERO & TAYLOR [1993] for the construction of an additive enhancement of the deformation gradient $\boldsymbol{F} := \text{GRAD}_X \boldsymbol{\varphi}$ at the element level. This procedure results in the expression

$$\boldsymbol{F}^h = \underbrace{\text{GRAD}_X \boldsymbol{\varphi}^h}_{conforming} + \underbrace{\tilde{\boldsymbol{F}}^h}_{enhanced} , \tag{2.3}$$

with the enhanced part $\tilde{\boldsymbol{F}}^h$ given by

$$\tilde{\boldsymbol{F}} = \boldsymbol{F}_o \, \tilde{\mathbb{F}} , \tag{2.4}$$

where $\boldsymbol{F}_o$ denotes the conforming part of the deformation gradient at the centroid

$$\boldsymbol{F}_o \equiv \text{GRAD}_0 \boldsymbol{\varphi}^h := \text{GRAD}_X \boldsymbol{\varphi}^h \Big|_{\boldsymbol{\xi}=\boldsymbol{0}} , \tag{2.5}$$

and $\tilde{\mathbb{F}}$ is a given enhanced interpolation field. This enhancement can be constructed as

$$\tilde{\mathbb{F}} = \frac{j_o}{j} \boldsymbol{J}_o \, \mathbb{F} \, \boldsymbol{J}_o^{-1} , \tag{2.6}$$

following the original formulation in SIMO & ARMERO [1992], or as

$$\tilde{\mathbb{F}} = \frac{j_o}{j} \boldsymbol{J}_o^{-T} \, \mathbb{F} \, \boldsymbol{J}_o^{-1} , \tag{2.7}$$

following GLASER & ARMERO [1995]. Here, $\boldsymbol{J}_o$ denotes the Jacobian of the isoparametric map $\boldsymbol{X} = \hat{\boldsymbol{X}}(\boldsymbol{\xi})$ at the centroid, i.e.,

$$\boldsymbol{J} = \boldsymbol{J}(\boldsymbol{\xi}) := \frac{\partial \hat{\boldsymbol{X}}}{\partial \boldsymbol{\xi}} , \quad \boldsymbol{J}_o = \boldsymbol{J}(\boldsymbol{\xi}) \Big|_{\boldsymbol{\xi}=\boldsymbol{0}} , \tag{2.8}$$

with determinants denoted by

$$j = j(\boldsymbol{\xi}) := \det \boldsymbol{J}(\boldsymbol{\xi}) , \quad j_o = j(\boldsymbol{\xi}) \Big|_{\boldsymbol{\xi}=\boldsymbol{0}} . \tag{2.9}$$

Note that both constructions (2.6) and (2.7) are frame indifferent under change of observer due to the presence of $\boldsymbol{F}_o$ in (2.4). We observe that for a reference undistorted element, as considered in the calculations below, $\boldsymbol{J}_o = \boldsymbol{1}$ and the two transformations (2.6) and (2.7) coincide.

The enhanced interpolations $\mathbb{F} = \mathbb{F}(\boldsymbol{\xi})$ are defined in the parent domain $\square$, and assumed of the form

$$\mathbb{F}(\boldsymbol{\xi}) = \sum_{I=1}^{n_{\text{enh}}} \mathbb{F}^I(\boldsymbol{\xi})\ \Gamma_I\ , \tag{2.10}$$

with n_{enh} enhanced parameters $\Gamma_I \in \mathbb{R}\ I = 1, n_{\text{enh}})$, ($n_{\text{enh}} = 4$ in the cases below). With this notation in hand, we consider the following elements for plane strain analyses:

1. *The Q1/E4 element.* The original formulation of SIMO & ARMERO [1992] is recovered by

$$\mathbb{F} = \Gamma_1 \begin{bmatrix} \xi & 0 \\ 0 & 0 \end{bmatrix} + \Gamma_2 \begin{bmatrix} 0 & 0 \\ \xi & 0 \end{bmatrix} + \Gamma_3 \begin{bmatrix} 0 & \eta \\ 0 & 0 \end{bmatrix} + \Gamma_4 \begin{bmatrix} 0 & 0 \\ 0 & \eta \end{bmatrix}\ . \tag{2.11}$$

   The transformation rule (2.6) is considered in this case.

2. *The Q1/ES4 element.* Numerical experiments (see below) have shown the presence of spurious zero energy modes in the original Q1/E4 element. To avoid these difficulties the following modification has been proposed in GLASER & ARMERO [1995]

$$\mathbb{F} = \Gamma_1 \begin{bmatrix} \xi & 0 \\ 0 & 0 \end{bmatrix} + \Gamma_2 \begin{bmatrix} 0 & \xi \\ \xi & 0 \end{bmatrix} + \Gamma_3 \begin{bmatrix} 0 & \eta \\ \eta & 0 \end{bmatrix} + \Gamma_4 \begin{bmatrix} 0 & 0 \\ 0 & \eta \end{bmatrix}\ , \tag{2.12}$$

   involving the symmetrization of (2.11). The transformation rule (2.6) is considered in this case.

3. *The Q1/ET4 element.* Numerical experiments show that the above modification suppresses the hourglass modes that appear for the Q1/E4 quad in compression. However, a stiff response of the element has been observed in bending dominated problems. To avoid this drawback, the following basis of the enhanced deformation gradient is considered

$$\mathbb{F} = \Gamma_1 \begin{bmatrix} \xi & 0 \\ 0 & 0 \end{bmatrix} + \Gamma_2 \begin{bmatrix} 0 & \xi \\ 0 & 0 \end{bmatrix} + \Gamma_3 \begin{bmatrix} 0 & 0 \\ \eta & 0 \end{bmatrix} + \Gamma_4 \begin{bmatrix} 0 & 0 \\ 0 & \eta \end{bmatrix}\ , \tag{2.13}$$

   involving the transpose of (2.11). The transformation (2.7) is considered in this case leading to an improved performance of the element.

Similar enhanced interpolations fields apply to the 3D and axisymmetric problems. See all the original references for details.

The three interpolation fields (2.11), (2.12) and (2.13) satisfy the condition

$$\int_{\square} \mathbb{F}\ d\square = 0\ , \tag{2.14}$$

proposed in SIMO & ARMERO [1992] for the element to satisfy the patch test. Constant strain states are captured exactly by the element with zero enhanced modes ($\Gamma_I = 0$,

$I = 1, 4$). We note that the purpose of considering the transformations (2.6) and (2.7), with the Jacobian $\boldsymbol{J}_o$ at the centroid of the element (i.e. constant) is precisely the satisfaction of the patch test in general distorted configurations of the element. These ideas were first proposed in TAYLOR et al. [1976] for the original infinitesimal incompatible modes element QM6.

2.2. The finite element equations

The weak form of the governing equations are written for a general hyperelastic material characterized by a stored energy function $W = W(\boldsymbol{F})$ as

$$\int_{\Omega^h} \Big[\partial_{\boldsymbol{F}} W : [\,\mathrm{GRAD}_X \delta\boldsymbol{\varphi}^h + \mathrm{GRAD}_0 \delta\boldsymbol{\varphi}^h \;\; \tilde{\mathbb{F}}]\Big] d\Omega - G_{ext}(\delta\boldsymbol{\varphi}^h) = 0 \,, \qquad (2.15.a)$$

$$\int_{\Omega^h} \partial_{\boldsymbol{F}} W : \boldsymbol{F}_o \; \delta\tilde{\mathbb{F}}] \; d\Omega = 0 \,, \qquad (2.15.b)$$

for all admissible variations $\delta\boldsymbol{\varphi}$ (satisfying homogeneous essential boundary conditions as usual), and all variations $\delta\tilde{\mathbb{F}}$. These equations can be obtained as the first variation of a three-field variational formulation of the Hu-Washizu type, with the proper orthogonality conditions for the stress field to drop out of the formulation. See the original references for details. In what follows, we use the notation

$$\boldsymbol{P} := \frac{\partial W}{\partial \boldsymbol{F}} \qquad \text{and} \qquad \boldsymbol{A} := \frac{\partial^2 W}{\partial \boldsymbol{F}^2} \,, \qquad (2.16)$$

for the first Piola-Kirchhoff stress tensor resulting from the stored energy function W and corresponding tangent, respectively.

The linearization of the weak equations (2.15) leads to a stiffness matrix $\boldsymbol{K}$ given by the expression

$$[\,\delta\boldsymbol{d} \quad \delta\boldsymbol{\Gamma}\,]\,\boldsymbol{K}\begin{bmatrix}\Delta\boldsymbol{d}\\ \Delta\boldsymbol{\Gamma}\end{bmatrix} = \int_{\Omega^h} \Big[[\delta\bar{\boldsymbol{F}} + \delta\boldsymbol{F}_o \;\tilde{\mathbb{F}} + \boldsymbol{F}_o \;\delta\tilde{\mathbb{F}}] : \boldsymbol{A} : [\Delta\bar{\boldsymbol{F}} + \Delta\boldsymbol{F}_o \;\tilde{\mathbb{F}} + \boldsymbol{F}_o \;\Delta\tilde{\mathbb{F}}]$$
$$+ \boldsymbol{P} : [\Delta\boldsymbol{F}_o \;\delta\tilde{\mathbb{F}} + \delta\boldsymbol{F}_o \;\Delta\tilde{\mathbb{F}}]\Big] d\Omega \,, \qquad (2.17)$$

where

$$\left.\begin{aligned}
&\Delta\bar{\boldsymbol{F}} := \mathrm{GRAD}_X[\Delta\boldsymbol{\varphi}^h] = \sum_{A=1}^{4} \Delta\boldsymbol{d}_A \otimes \mathrm{GRAD}_X N^A \,,\\
&\Delta\boldsymbol{F}_o := \Delta\bar{\boldsymbol{F}}\Big|_{\boldsymbol{\xi}=0} \,,\\
&\Delta\tilde{\mathbb{F}} = \sum_{I=1}^{4} \Delta\mathbb{F}^I \boldsymbol{\Gamma}_I \,,\\
&\Delta\boldsymbol{d} = [\,\Delta\boldsymbol{d}_1^T \quad \Delta\boldsymbol{d}_2^T \quad \Delta\boldsymbol{d}_3^T \quad \Delta\boldsymbol{d}_4^T\,]^T \,,\\
&\Delta\boldsymbol{\Gamma} = [\,\Delta\boldsymbol{\Gamma}_1 \quad \Delta\boldsymbol{\Gamma}_2 \quad \Delta\boldsymbol{\Gamma}_3 \quad \Delta\boldsymbol{\Gamma}_4\,]^T \,,
\end{aligned}\right\} \qquad (2.18)$$

and similarly for the $\delta[\cdot]$ variations. It is to be noted that, since the enhanced parameters Γ_I are defined independently for each element, an efficient numerical implementation involves their static condensation at the element level leading to an effective (8×8) stiffness of the element. See SIMO & ARMERO [1992] for completed details, and the considerations in Section 3 below.

2.2.1. The material tangent

We consider a general Ogden material model characterized by a stored energy function in terms of the principal stretches $\{\lambda_1, \lambda_2\}$ ($\lambda_3 = 1$ in plane strain). The principal second Piola-Kirchhoff stresses S_A $(A = 1, 2)$ are given by

$$S_A = \frac{1}{\lambda_A}\frac{\partial W}{\partial \lambda_A} \qquad \text{(no sum in } A) \,, \tag{2.19}$$

and, denoting the Lagrangian principal directions $\boldsymbol{N}_A$, we have the formulas

$$\boldsymbol{S} = \sum_{A=1}^{2} S_A \boldsymbol{N}_A \otimes \boldsymbol{N}_A \,, \quad \text{with} \qquad \boldsymbol{P} = \boldsymbol{F}\boldsymbol{S} \,, \tag{2.20}$$

for the (in-plane) second and first Piola-Kirchhoff stresses, respectively. The material tangent $d\boldsymbol{S} = \mathbb{C}\frac{1}{2}d\boldsymbol{C}$ (with the right Cauchy-Green tensor $\boldsymbol{C} = \boldsymbol{F}^T\boldsymbol{F}$) is given by

$$\begin{aligned}\mathbb{C} = &\sum_{A,B} \frac{1}{\lambda_A}\frac{\partial}{\partial \lambda_A}\Big[\frac{1}{\lambda_B}\frac{\partial W}{\partial \lambda_B}\Big]\boldsymbol{N}_A \otimes \boldsymbol{N}_A \otimes \boldsymbol{N}_B \otimes \boldsymbol{N}_B \\ &+ \sum_{A \neq B} 2\,\frac{\lambda_A^2 S_A - \lambda_B^2 S_B}{\lambda_A^2 - \lambda_B^2}\,\tfrac{1}{2}(\boldsymbol{N}_A \otimes \boldsymbol{N}_B + \boldsymbol{N}_B \otimes \boldsymbol{N}_A) \otimes \tfrac{1}{2}(\boldsymbol{N}_A \otimes \boldsymbol{N}_B + \boldsymbol{N}_B \otimes \boldsymbol{N}_A) \,. \end{aligned} \tag{2.21}$$

From this last expression, we can identify the components of the material tangent $\mathbb{C}$ in the Lagrangian principal frame

$$C_{AABB} = \frac{1}{\lambda_A}\frac{\partial}{\partial \lambda_A}\Big[\frac{1}{\lambda_B}\frac{\partial W}{\partial \lambda_B}\Big] \,, \qquad C_{ABAB} = C_{ABBA} = \frac{\lambda_A^2 S_A - \lambda_B^2 S_B}{\lambda_A^2 - \lambda_B^2} \quad (A \neq B) \,, \tag{2.22}$$

where no sum over repeated indices is implied. The expression $(2.22)_2$ assumes different principal stretches. In the case of $\lambda_1 = \lambda_2$, this last expression is replaced by

$$C_{ABBA} = C_{ABAB} = \frac{\partial}{\partial \lambda_A^2}\left(\lambda_A^2 S_A - \lambda_B^2 S_B\right) \,, \tag{2.23}$$

with λ_A being equal to λ_B after differentiation. The tangent $\boldsymbol{A}$ in $(2.16)_2$ is obtained by

$$A^{iBkD} = F_A^i F_C^k C^{ABCD} + S^{BD}\delta^{ik} \,. \tag{2.24}$$

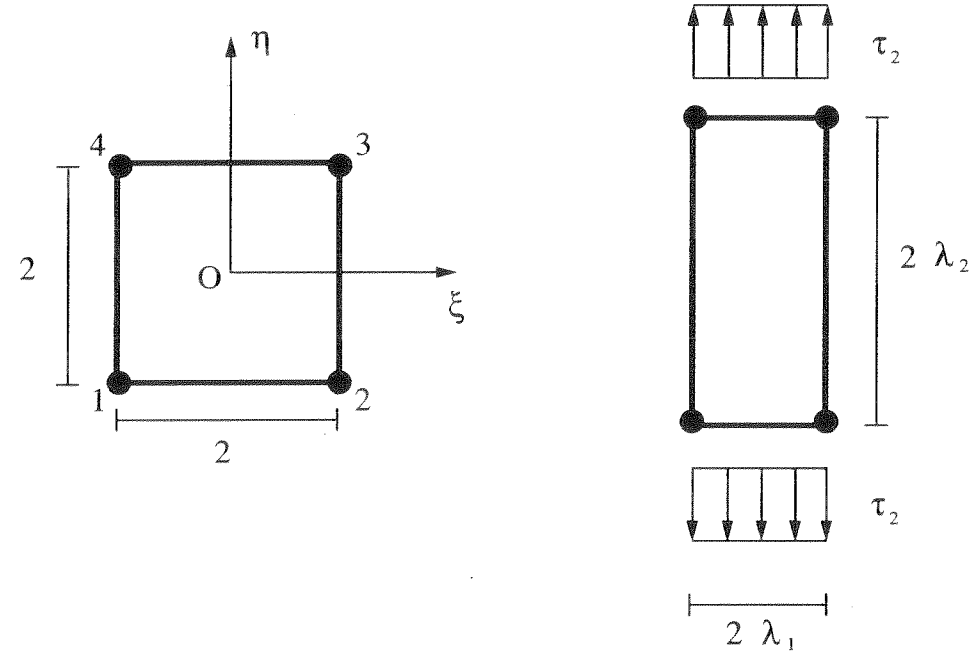

FIGURE 2.1. Undistorted single element test under uniaxial tension/compression state of stress.

The reader is referred to OGDEN [1983], Section 6.1.4, for details on all the formulas above.

The case of interest herein corresponds to an Ogden hyperelastic model of the form

$$W(\lambda_1, \lambda_2) = U(J) + \frac{\mu}{\alpha}\left[\lambda_1^\alpha + \lambda_2^\alpha - 2\right] - \mu \ln J \,, \tag{2.25}$$

for a volumetric response function $U(J)$ in terms of the Jacobian $J := \lambda_1\lambda_2$. A state of uniaxial tension in the 2-direction, characterized by a deformation gradient of the form

$$\boldsymbol{F} = \begin{bmatrix} \lambda_1 & 0 \\ 0 & \lambda_2 \end{bmatrix} \,, \tag{2.26}$$

is considered. The principal directions $\boldsymbol{N}_A$ are then the two Cartesian directions of reference. Setting the Kirchhoff stress $\tau_1 := S_1\lambda_1^2 = 0$, we obtain

$$\tau_1 = JU' + \mu(\lambda_1^\alpha - 1) = 0 \quad \Longrightarrow \quad JU' = -\mu(\lambda_1^\alpha - 1) \,, \tag{2.27}$$

and conclude that

$$\tau_2 := S_2\lambda_2^2 = JU' + \mu(\lambda_2^\alpha - 1) = \mu(\lambda_2^\alpha - \lambda_1^\alpha) \,. \tag{2.28}$$

See Figure 2.1 for an illustration of this state of stress. In this case, the tangent $\boldsymbol{A}$ is given

in components as

$$\left.\begin{aligned}
&A_{1111} = \frac{(JU')'}{\lambda_1^2} + \mu\frac{\alpha\lambda_1^\alpha}{\lambda_1^2}\,,\\
&A_{2222} = \frac{(JU')'}{\lambda_2^2} + \mu\frac{(\alpha+1)\lambda_2^\alpha + \lambda_1^\alpha}{\lambda_2^2}\,,\\
&A_{1122} = A_{2211} = \frac{(JU')'}{\lambda_1\lambda_2}\,,\\
&A_{1212} = A_{2121} = \mu\frac{\lambda_2^\alpha - \lambda_1^\alpha}{\lambda_2^2 - \lambda_1^2}\,,\\
&A_{1221} = A_{2112} = \mu\frac{\lambda_2^\alpha - \lambda_1^\alpha}{\lambda_2^2 - \lambda_1^2}\,\frac{\lambda_1}{\lambda_2}\,,\\
&A_{ABAA} = A_{ABBB} = A_{AABA} = A_{BBAB} = 0 \qquad (A \neq B)\,,
\end{aligned}\right\} \tag{2.29}$$

after some simple manipulations. Furthermore, equation $(2.27)_2$ allows to obtain a closed form expression of the transversal stretch λ_1 in term of the axial stretch λ_2.

In the numerical examples considered in Section 4, the particular volumetric response

$$U(J) = \tfrac{1}{2}\Lambda(\ln J)^2\,, \tag{2.30}$$

is considered. In this case, the volumetric contribution to the tangent in (2.29) is given by

$$(JU')' = \Lambda\,, \tag{2.31}$$

and equation (2.27) leads to the relation

$$\lambda_2 = \frac{1}{\lambda_1}\exp[-\frac{\mu}{\Lambda}(\lambda_1^\alpha - 1)]\,, \tag{2.32}$$

between λ_1 and λ_2.

3. Modal Analysis

We particularize the above developments to a single undistorted finite element occupying the parent domain as in WRIGGERS & REESE [1995], i.e. $\Omega^h = \square = [-1,1] \times [-1,1]$. The element is assumed to be subjected to a homogeneous deformation consisting of a uniform axial tension in the η direction (2-direction), leading to $\boldsymbol{F} = \boldsymbol{F}_o$ given by (2.26); see Figure 2.1. In this situation, the enhanced parameters $\Gamma^I = 0$ $(I = 1, n_{\text{enh}})$, since the element is designed to capture exactly constant states of deformation (patch test) by imposing (2.14).

We introduce the vector notation

$$\Delta \boldsymbol{P} \longrightarrow \Delta \boldsymbol{P} = \begin{bmatrix} P_{11} \\ P_{22} \\ P_{12} \\ P_{21} \end{bmatrix} \qquad \text{and} \qquad \Delta \boldsymbol{F} \longrightarrow \Delta \boldsymbol{F} = \begin{bmatrix} \Delta F_{11} \\ \Delta F_{22} \\ \Delta F_{12} \\ \Delta F_{21} \end{bmatrix} , \tag{3.1}$$

where, for simplicity, we use the same symbol for the tensor and corresponding matrix. Using the relations (2.29), we can write

$$\begin{bmatrix} \Delta P_{11} \\ \Delta P_{22} \\ \Delta P_{12} \\ \Delta P_{21} \end{bmatrix} = \underbrace{\begin{bmatrix} \boldsymbol{A}^n & \boldsymbol{0} \\ \boldsymbol{0} & \boldsymbol{A}^s \end{bmatrix}}_{:= \boldsymbol{A}} \begin{bmatrix} \Delta F_{11} \\ \Delta F_{22} \\ \Delta F_{12} \\ \Delta F_{21} \end{bmatrix} , \tag{3.2}$$

where we have introduced the notation

$$\boldsymbol{A}^n := \frac{(JU')'}{\lambda_1 \lambda_2} \begin{bmatrix} \frac{\lambda_2}{\lambda_1} & 1 \\ 1 & \frac{\lambda_1}{\lambda_2} \end{bmatrix} + \begin{bmatrix} \mu\alpha\lambda_1^{\alpha-2} & 0 \\ \mu 0 & \frac{(\alpha+1)\lambda_2^\alpha + \lambda_1^\alpha}{\lambda_2^2} \end{bmatrix} , \tag{3.3}$$

$$\boldsymbol{A}^s := \mu \frac{\lambda_2^\alpha - \lambda_1^\alpha}{\lambda_2^2 - \lambda_1^2} \begin{bmatrix} 1 & \frac{\lambda_1}{\lambda_2} \\ \frac{\lambda_1}{\lambda_2} & 1 \end{bmatrix} , \tag{3.4}$$

for the material constants involving the normal and shear components.

With this notation in hand, we can write for the case of interest

$$\Delta \bar{\boldsymbol{F}} = [\mathbb{P}_{cons} + \boldsymbol{B}\mathbb{P}_{hour}]\, \Delta \boldsymbol{d} , \tag{3.5}$$

after some straightforward manipulations, where

$$\left.\begin{aligned} \mathbb{P}_{cons} &:= \frac{1}{4} \begin{bmatrix} -1 & 0 & 1 & 0 & 1 & 0 & -1 & 0 \\ 0 & -1 & 0 & -1 & 0 & 1 & 0 & 1 \\ -1 & 0 & -1 & 0 & 1 & 0 & 1 & 0 \\ 0 & -1 & 0 & 1 & 0 & 1 & 0 & -1 \end{bmatrix} , \\ \mathbb{P}_{hour} &:= \frac{1}{4} \begin{bmatrix} 1 & 0 & -1 & 0 & 1 & 0 & -1 & 0 \\ 0 & 1 & 0 & -1 & 0 & 1 & 0 & -1 \end{bmatrix} , \\ \boldsymbol{B} &:= \begin{bmatrix} \eta & 0 \\ 0 & \xi \\ \xi & 0 \\ 0 & \eta \end{bmatrix} , \end{aligned}\right\} \tag{3.6}$$

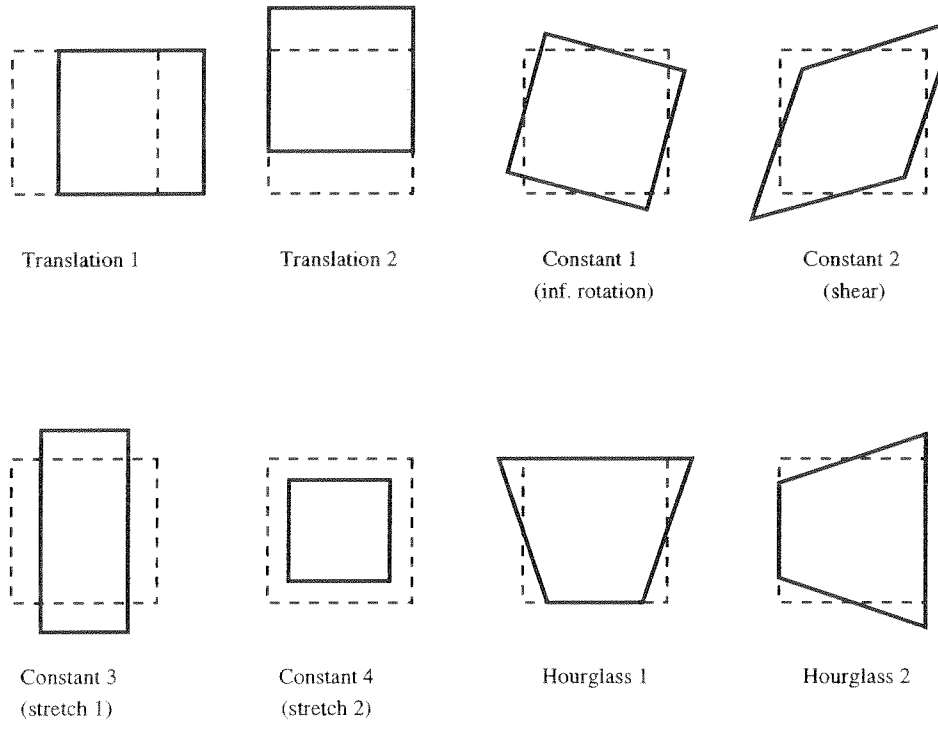

FIGURE 3.1. The eight modes of an undistorted square element: two translations, one infinitesimal rotation, one shear, two stretchings (infinitesimally isochoric in the incompressible limit, and otherwise), and two hourglass modes.

Remark 3.1. We also introduce the matrix

$$\mathbb{P}_{trans} := \frac{1}{4}\begin{bmatrix} 1 & 0 & 1 & 0 & 1 & 0 & 1 & 0 \\ 0 & 1 & 0 & 1 & 0 & 1 & 0 & 1 \end{bmatrix} , \tag{3.7}$$

and observe that the three matrices $\mathbb{P}_{cons}$, $\mathbb{P}_{hour}$, and $\mathbb{P}_{trans}$ have full rank

$$\text{rank}\,[\mathbb{P}_{hour}] = \text{rank}\,[\mathbb{P}_{trans}] = 2 , \qquad \text{rank}\,[\mathbb{P}_{cons}] = 4 \tag{3.8}$$

In fact, the rows of these three matrices are orthogonal, and span $\mathbb{R}^8$. We also conclude that

$$\begin{aligned} \text{Ker}\,[\mathbb{P}_{cons}] &= \text{span}\{\text{rows of } \mathbb{P}_{hour} \text{ and } \mathbb{P}_{trans}\} , \\ \text{Ker}\,[\mathbb{P}_{hour}] &= \text{span}\{\text{rows of } \mathbb{P}_{cons} \text{ and } \mathbb{P}_{trans}\} , \end{aligned} \tag{3.9}$$

hence

$$\text{Ker}\,[\mathbb{P}_{cons}] \cap \text{Ker}\,[\mathbb{P}_{hour}] = \text{span}\{\text{rows of } \mathbb{P}_{trans}\} . \tag{3.10}$$

We introduce the following vectors for the developments that follow

$$\Delta \boldsymbol{d}_1^{cons} = \frac{1}{4}\begin{bmatrix} -1 \\ 1 \\ -1 \\ -1 \\ 1 \\ -1 \\ 1 \\ 1 \end{bmatrix}, \quad \Delta \boldsymbol{d}_2^{cons} = \frac{1}{4}\begin{bmatrix} -1 \\ -1 \\ -1 \\ 1 \\ 1 \\ 1 \\ 1 \\ -1 \end{bmatrix}, \quad \Delta \boldsymbol{d}_1^{hour} = \frac{1}{4}\begin{bmatrix} 1 \\ 0 \\ -1 \\ 0 \\ 1 \\ 0 \\ -1 \\ 0 \end{bmatrix}, \quad \Delta \boldsymbol{d}_2^{hour} = \frac{1}{4}\begin{bmatrix} 0 \\ 1 \\ 0 \\ -1 \\ 0 \\ 1 \\ 0 \\ -1 \end{bmatrix}, \tag{3.11}$$

and

$$\Delta \boldsymbol{d}_1^{trans} = \frac{1}{4}\begin{bmatrix} 1 \\ 0 \\ 1 \\ 0 \\ 1 \\ 0 \\ 1 \\ 0 \end{bmatrix}, \quad \Delta \boldsymbol{d}_2^{trans} = \frac{1}{4}\begin{bmatrix} 0 \\ 1 \\ 0 \\ 1 \\ 0 \\ 1 \\ 0 \\ 1 \end{bmatrix}. \tag{3.12}$$

We can identify $\Delta \boldsymbol{d}_i^{hour}$ and $\Delta \boldsymbol{d}_i^{trans}$ as the rows of $\mathbb{P}_{hour}$ and $\mathbb{P}_{trans}$, respectively. Physically, the nodal incremental displacements $\Delta \boldsymbol{d}_1^{cons}$ correspond to an infinitesimal rotation, $\Delta \boldsymbol{d}_2^{cons}$ corresponds to the shearing mode, whereas $\Delta \boldsymbol{d}_1^{hour}$ and $\Delta \boldsymbol{d}_2^{hour}$ correspond to an hourglass pattern in the 1 and 2-directions, respectively. This modes are represented in Figure 3.1. The stretching modes $\Delta \boldsymbol{d}_3^{cons}$ and $\Delta \boldsymbol{d}_4^{cons}$ are identified below. ■

The enhanced part of the deformation gradient can be written as

$$\boldsymbol{F}_o \Delta\tilde{\mathbb{F}} = \left\{ \begin{bmatrix} \lambda_1\xi & 0 \\ 0 & 0 \end{bmatrix}, \begin{bmatrix} 0 & \hat{\lambda}_1\xi \\ \tilde{\lambda}_2\xi & 0 \end{bmatrix}, \begin{bmatrix} 0 & \tilde{\lambda}_1\eta \\ \hat{\lambda}_2\eta & 0 \end{bmatrix}, \begin{bmatrix} 0 & 0 \\ 0 & \lambda_2\eta \end{bmatrix} \right\} \begin{bmatrix} \Delta\Gamma_1 \\ \Delta\Gamma_2 \\ \Delta\Gamma_3 \\ \Delta\Gamma_4 \end{bmatrix}, \tag{3.13}$$

which, in the vector notation defined by (3.2), reads

$$\boldsymbol{F}_o \Delta\tilde{\mathbb{F}} = \boldsymbol{G}\Delta\boldsymbol{\Gamma}, \qquad \text{with} \quad \boldsymbol{G} = \begin{bmatrix} \lambda_1\xi & 0 & 0 & 0 \\ 0 & \hat{\lambda}_1\xi & \tilde{\lambda}_1\eta & 0 \\ 0 & \tilde{\lambda}_2\xi & \hat{\lambda}_2\eta & 0 \\ 0 & 0 & 0 & \lambda_2\eta \end{bmatrix}. \tag{3.14}$$

Here we have introduced the symbols $\hat{\lambda}_i$ and $\tilde{\lambda}_i$ $(i = 1, 2)$ to track the contributions of the different terms in the final expressions. The different elements described in Section 2 are recovered as follows:

1. Q1/E4: $\tilde{\lambda}_i = \lambda_i$ and $\hat{\lambda}_i = 0$ $(i = 1, 2)$.

2. Q1/ES4: $\tilde{\lambda}_i = \lambda_i$ and $\hat{\lambda}_i = \lambda_i$ $(i = 1, 2)$.

3. Q1/ET4: $\tilde{\lambda}_i = 0$ and $\hat{\lambda}_i = \lambda_i$ $(i = 1, 2)$.

With this notation, the stiffness matrix $\boldsymbol{K}$ (12×12) is expressed as follows

$$\boxed{\boldsymbol{K} = \begin{bmatrix} \mathbb{P}_{cons}^T \boldsymbol{K}_{11}^{cons} \mathbb{P}_{cons} & \boldsymbol{0} \\ \boldsymbol{0} & \boldsymbol{0} \end{bmatrix} + \begin{bmatrix} \mathbb{P}_{hour}^T \boldsymbol{K}_{11}^{hour} \mathbb{P}_{hour} & \mathbb{P}_{hour}^T \boldsymbol{K}_{12}^{hour} \\ \boldsymbol{K}_{12}^{hour\,T} \mathbb{P}_{hour} & \boldsymbol{K}_{22}^{hour} \end{bmatrix}}, \tag{3.15}$$

where

$$\boldsymbol{K}_{11}^{cons} = \int_\Omega \boldsymbol{A}\, d\Omega = 4\, \boldsymbol{A}_{(4\times 4)}\,, \tag{3.16}$$

$$\boldsymbol{K}_{11}^{hour} = \int_\Omega \boldsymbol{B}^T \boldsymbol{A} \boldsymbol{B}\, d\Omega = \frac{4}{3} \begin{bmatrix} A_{11}^n + A_{11}^s & 0 \\ 0 & A_{22}^n + A_{22}^s \end{bmatrix}_{(2\times 2)}, \tag{3.17}$$

$$\begin{aligned} \boldsymbol{K}_{12}^{hour} &= \int_\Omega \boldsymbol{B}^T \boldsymbol{A} \boldsymbol{G}\, d\Omega \\ &= \frac{4}{3} \begin{bmatrix} 0 & A_{11}^s \hat{\lambda}_1 + A_{12}^s \tilde{\lambda}_2 & 0 & A_{12}^n \lambda_2 \\ A_{21}^n \lambda_1 & 0 & A_{21}^s \tilde{\lambda}_1 + A_{22}^s \hat{\lambda}_2 & 0 \end{bmatrix}_{(2\times 4)}, \end{aligned} \tag{3.18}$$

$$\begin{aligned} \boldsymbol{K}_{22}^{hour} &= \int_\Omega \boldsymbol{G}^T \boldsymbol{A} \boldsymbol{G}\, d\Omega \\ &= \frac{4}{3} \begin{bmatrix} A_{11}^n \lambda_1^2 & 0 & 0 & 0 \\ 0 & \begin{matrix} \hat{\lambda}_1 \left[A_{11}^s \hat{\lambda}_1 + A_{12}^s \tilde{\lambda}_2 \right] \\ +\tilde{\lambda}_2 \left[A_{21}^s \hat{\lambda}_1 + A_{22}^s \tilde{\lambda}_2 \right] \end{matrix} & 0 & 0 \\ 0 & 0 & \begin{matrix} \tilde{\lambda}_1 \left[A_{11}^s \tilde{\lambda}_1 + A_{12}^s \hat{\lambda}_2 \right] \\ +\hat{\lambda}_2 \left[A_{21}^s \tilde{\lambda}_1 + A_{22}^s \hat{\lambda}_2 \right] \end{matrix} & 0 \\ 0 & 0 & 0 & A_{22}^n \lambda_2^2 \end{bmatrix}_{(4\times 4)} \end{aligned} \tag{3.19}$$

Finally, the enhanced degrees of freedom $\boldsymbol{\Gamma}$ are eliminated at the element level, leading to the statically condensed stiffness matrix

$$\boxed{\boldsymbol{K}^\star_{(8\times 8)} = \mathbb{P}_{cons}^T \boldsymbol{K}_{11}^{cons} \mathbb{P}_{cons} + \mathbb{P}_{hour}^T \underbrace{\left[\boldsymbol{K}_{11}^{hour} - \boldsymbol{K}_{12}^{hour} (\boldsymbol{K}_{22}^{hour})^{-1} \boldsymbol{K}_{12}^{hour\,T} \right]}_{:= \boldsymbol{K}^{*,hour}} \mathbb{P}_{hour}}, \tag{3.20}$$

After some manipulations, we obtain

$$\boxed{\boldsymbol{K}^{*,hour} = 4 \begin{bmatrix} \omega_1^{hour} & 0 \\ 0 & \omega_2^{hour} \end{bmatrix}}, \tag{3.21}$$

where

$$\boxed{\begin{aligned}\omega_1^{hour} &= \frac{1}{3}\left[A_{11}^n - \frac{\left(A_{12}^n\right)^2}{A_{22}^n} + A_{11}^s - \frac{\left(A_{11}^s\hat{\lambda}_1 + A_{12}^s\tilde{\lambda}_2\right)^2}{\hat{\lambda}_1\left[A_{11}^s\hat{\lambda}_1 + A_{12}^s\tilde{\lambda}_2\right] + \tilde{\lambda}_2\left[A_{21}^s\hat{\lambda}_1 + A_{22}^s\tilde{\lambda}_2\right]}\right], \\ \omega_2^{hour} &= \frac{1}{3}\left[A_{22}^n - \frac{\left(A_{21}^n\right)^2}{A_{11}^n} + A_{22}^s - \frac{\left(A_{21}^s\tilde{\lambda}_1 + A_{22}^s\hat{\lambda}_2\right)^2}{\tilde{\lambda}_1\left[A_{11}^s\tilde{\lambda}_1 + A_{12}^s\hat{\lambda}_2\right] + \hat{\lambda}_2\left[A_{21}^s\tilde{\lambda}_1 + A_{22}^s\hat{\lambda}_2\right]}\right].\end{aligned}} \tag{3.22}$$

Examination of (3.20) and after the considerations in Remark 3.1, we identify ω_1^{hour} and ω_2^{hour} as the eigenvalues of $\boldsymbol{K}^*$ corresponding to the eigenvectors $\Delta\boldsymbol{d}_1^{hour}$ and $\Delta\boldsymbol{d}_2^{hour}$ in (3.11), respectively. These are the *two hourglass modes* of the element.

The constant part of the stiffness matrix contributes with the 4 constant modes of $\boldsymbol{K}_{11}^{cons} = 4\boldsymbol{A}$. These eigenvalues can be obtained with a simple calculation involving the 2×2 matrices $\boldsymbol{A}^n$ and $\boldsymbol{A}^s$. The contributions of $\boldsymbol{A}^s$ are

$$\boxed{\begin{aligned}\omega_1^{cons} &= \tfrac{1}{2}\left[(A_{11}^s + A_{22}^s) - \sqrt{\left(A_{11}^s - A_{22}^s\right)^2 + 4A_{12}^s A_{21}^s}\,\right] = \frac{\mu}{\lambda_2}\frac{\lambda_2^\alpha - \lambda_1^\alpha}{\lambda_2 + \lambda_1}, \\ \omega_2^{cons} &= \tfrac{1}{2}\left[(A_{11}^s + A_{22}^s) + \sqrt{\left(A_{11}^s - A_{22}^s\right)^2 + 4A_{12}^s A_{21}^s}\,\right] = \frac{\mu}{\lambda_2}\frac{\lambda_2^\alpha - \lambda_1^\alpha}{\lambda_2 - \lambda_1},\end{aligned}} \tag{3.23}$$

with the corresponding eigenvectors given by $\Delta\boldsymbol{d}_1^{cons}$ and $\Delta\boldsymbol{d}_2^{cons}$ of (3.11), respectively. The ω_1^{cons} corresponds to the (infinitesimal) rigid rotation, and we observe that it does not vanish unless $\lambda_1 = \lambda_2$, i.e. in the undeformed state in the case of interest. This eigenvalue is positive in uniaxial tension $\lambda_1 < 1$, $\lambda_2 > 1$, and negative in uniaxial compression $\lambda_1 > 1$, $\lambda_2 < 1$. On the other hand, the eigenvalue ω_2^{cons} corresponds to the *shearing mode*, and it has the value $\alpha\mu$ in the undeformed configuration.

The two contributions of the normal components $\boldsymbol{A}^n$ of the tangent are given by

$$\boxed{\begin{aligned}\omega_3^{cons} &= \tfrac{1}{2}\left[(A_{11}^n + A_{22}^n) - \sqrt{\left(A_{11}^n - A_{22}^n\right)^2 + 4A_{12}^n A_{21}^n}\,\right], \\ \omega_4^{cons} &= \tfrac{1}{2}\left[(A_{11}^n + A_{22}^n) + \sqrt{\left(A_{11}^n - A_{22}^n\right)^2 + 4A_{12}^n A_{21}^n}\,\right],\end{aligned}} \tag{3.24}$$

corresponding to the stretching modes. The corresponding eigenvectors are obtained as

$$\Delta \boldsymbol{d}_i^{cons} = \frac{1}{4}\begin{bmatrix} 1 \\ -b_i \\ -1 \\ -b_i \\ -1 \\ b_i \\ 1 \\ b_i \end{bmatrix}, \qquad \text{where} \quad b_i = \frac{\lambda_2}{\lambda_1}\left[1 + \frac{\mu}{\Lambda}\alpha\lambda_1^{\alpha} - \frac{\omega_i^{cons}}{\Lambda}\lambda_1^2\right], \tag{3.25}$$

for $i = 3, 4$. We observe that in the incompressible limit $\Lambda \to \infty$ ($\Rightarrow \lambda_1 \to \lambda_2^{-1}$ by (2.32)) these two eigenvalues are such that $\omega_4^{cons} \to \infty$ and ω_3 remains finite (infinitesimally isochoric stretching), with the eigenvectors given by

$$\Delta \boldsymbol{d}_3^{cons} = \frac{1}{4}\begin{bmatrix} 1 \\ -\frac{\lambda_2}{\lambda_1} \\ -1 \\ -\frac{\lambda_2}{\lambda_1} \\ -1 \\ \frac{\lambda_2}{\lambda_1} \\ 1 \\ \frac{\lambda_2}{\lambda_1} \end{bmatrix}, \text{ and } \quad \Delta \boldsymbol{d}_4^{cons} = \frac{1}{4}\begin{bmatrix} 1 \\ \frac{\lambda_1}{\lambda_2} \\ -1 \\ \frac{\lambda_1}{\lambda_2} \\ -1 \\ -\frac{\lambda_1}{\lambda_2} \\ 1 \\ -\frac{\lambda_1}{\lambda_2} \end{bmatrix}. \tag{3.26}$$

A simple calculation shows that the infinitesimal strain associated to the incremental nodal displacements $\Delta \boldsymbol{d}_3^{cons}$ is isochoric. The two stretching modes given by $(3.25)_1$ are shown in Figure 3.1.

Finally, the set of element eigenvalues is completed with the two translational modes $\omega_1^{trans} = \omega_2^{trans} = 0$ with eigenvectors given by $\Delta \boldsymbol{d}_1^{trans}$ and $\Delta \boldsymbol{d}_2^{trans}$ as given by (3.12). These modes correspond to the translation in the 1 and 2 directions, respectively.

Remark 3.2. As expected, the homogeneous deformation modes ω_i^{cons} $(i = 1, 4)$, and the two translational modes $\omega_i^{trans} = 0$ $(i = 1, 2)$ are captured exactly by all the elements since they all pass the patch test. Constant state of stresses are represented exactly by the elements. ■

4. Discussion of results

We first consider the case of a Neo-Hookean model, characterized by $\alpha = 2$. A value of $\Lambda/\mu = 10^5/20$ is considered, leading effectively to the quasi-incompressible

a)

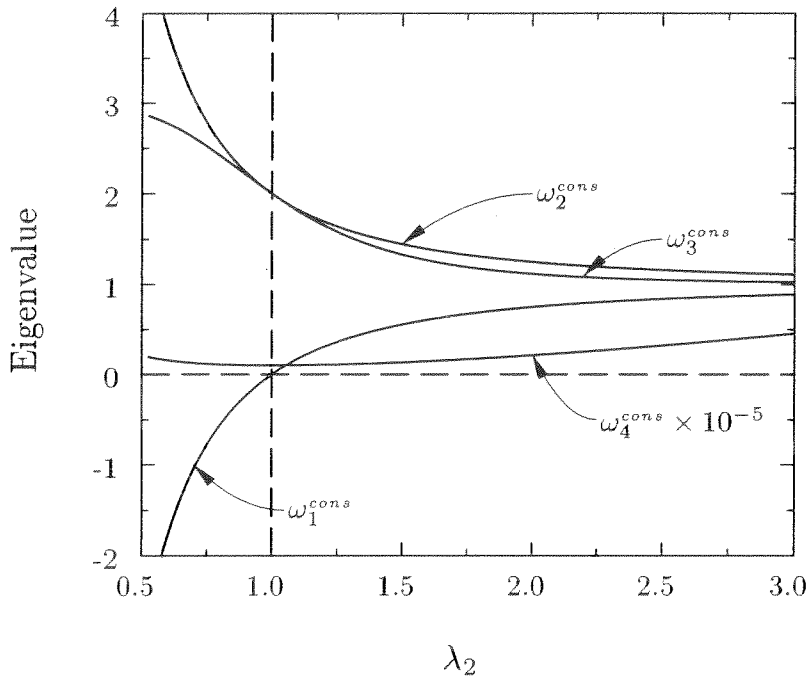

b)

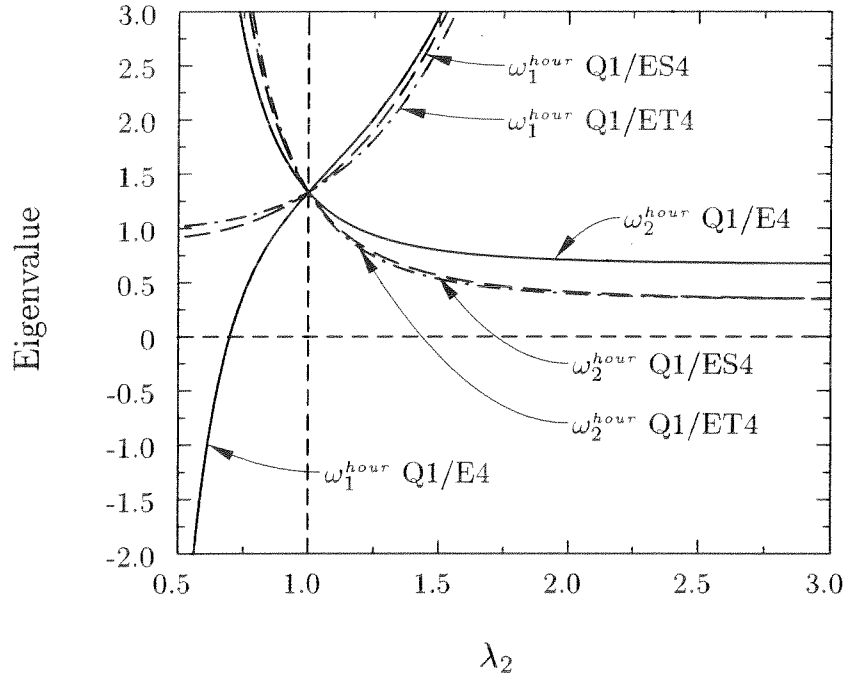

FIGURE 3.2. Neo-Hookean model $\alpha = 2.0$, $\Lambda/\mu = 10^5/20$. **a)** Homogeneous deformation modes for all the elements: ω_1^{cons}, infinitesimal rotation; ω_2^{cons}, shearing; ω_3^{cons}, isochoric stretching; and ω_4^{cons}, volumetric (note the scaling). **b)** Hourglass modes for the different elements. Note the negative eigenvalue of the Q1/E4 in compression.

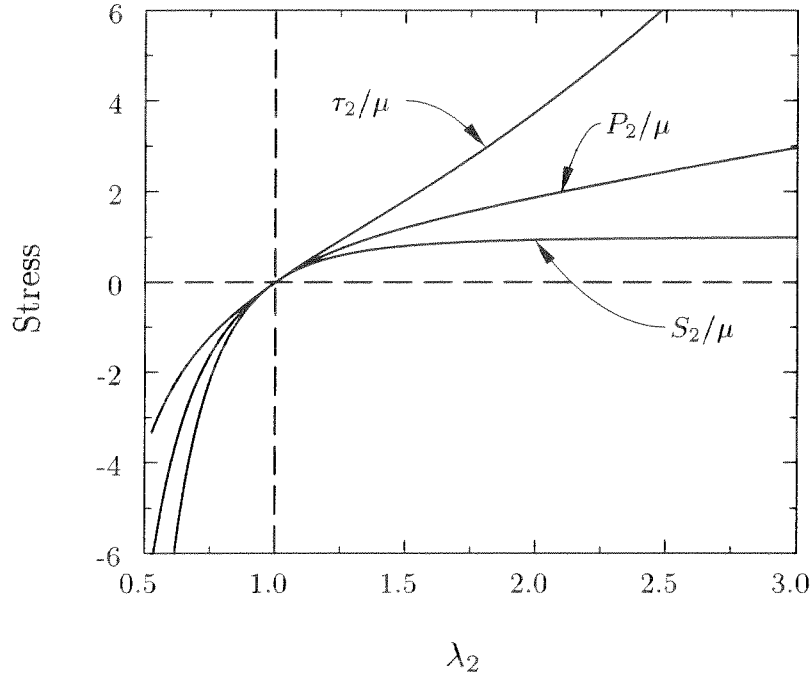

FIGURE 3.3. Neo-Hookean model $\alpha = 2.0$, $\Lambda/\mu = 10^5/20$. Axial Kirchhoff stress (τ_2), second Piola-Kirchhoff stress ($S_2 = \tau_2/\lambda_2^2$), and nominal axial stress ($P_2 = \tau_2/\lambda_2$, first Piola-Kirchhoff stress).

range. Figure 3.2.a depicts the eigenvalues ω_i^{cons} $(i = 1, 4)$ associated to the constant strain modes for this case. As observed above, the eigenvalue ω_1^{cons} corresponding to an infinitesimal rotation is negative in compression and positive in tension. Note the scaling of the volumetric mode ω_4^{cons}. As indicated in Remark 3.2, since all the elements pass the patch test, these four modes (and the two translational zero modes) are captured exactly by all the elements. Figure 3.2.b depicts the eigenvalues associated to the two hourglass modes for the three different elements Q1/E4, Q1/ES4, and Q1/ET4. Clearly, the original Q1/E4 shows a negative eigenvalue (passing through a zero energy mode) in compression, confirming the results of WRIGGERS & REESE [1995].

Particularizing expression (3.22) to the Q1/E4 element ($\tilde{\lambda}_i = \lambda_i$, $\hat{\lambda}_i = 0$, $i = 1, 2$), we observe

$$(\omega_1^{hour})_{Q1/E4} = \frac{1}{3}\left[\frac{\det \boldsymbol{A}^n}{A_{22}^n} + \frac{\det \boldsymbol{A}^s}{A_{22}^s}\right] , \tag{4.1}$$

where

$$\det \boldsymbol{A}^n/A^n_{22} = \left[\frac{\frac{\mu}{\Lambda}\left[(\alpha+1)\lambda_1^\alpha + (\alpha-1)\lambda_1^\alpha\right] + \alpha\left(\frac{\mu}{\Lambda}\right)^2\lambda_1^\alpha\left[\lambda_1^\alpha + \lambda_2^\alpha(\alpha-1)\right]}{\lambda_1^2\left[1+\frac{\mu}{\Lambda}\Big((\alpha+1)\lambda_2^\alpha + \lambda_1^\alpha\Big)\right]}\right]_{\alpha=2} > 0, \quad (4.2)$$

$$\det \boldsymbol{A}^s/A^s_{22} = \left[\frac{\mu\alpha}{\lambda_2^2}\left(\lambda_2^\alpha - \lambda_1^\alpha\right)\right]_{\alpha=2} < 0 \text{ in compression}, \quad > 0 \text{ in tension}. \quad (4.3)$$

Clearly ω_1^{hour} becomes negative because $\det \boldsymbol{A}^s < 0$ in compression, that is, because infinitesimal rotations have negative stiffness in uniaxial compression. This mode corresponds to hourglassing (bending) in the 1-direction (transversal to the load), as given by $\Delta \boldsymbol{d}_1^{hour}$. The Q1/ES4 and Q1/ET4 elements do not exhibit this zero energy mode. Figure 3.3 includes the axial stress/axial stretch relations for the Kirchhoff stress τ_2, nominal stress $P_2 = \tau_2/\lambda_2$ (first Piola-Kirchhoff stress), and the second Piola-Kirchhoff principal stress $S_2 = \tau_2/\lambda_2^2$, for this case.

We note that in the infinitesimal case ($\lambda_1 = \lambda_2 = 1$) all the elements reduce to the same element, the infinitesimal QM6 element of TAYLOR et al [1976]. In this case, the contribution of $\boldsymbol{A}^s$ to the stiffness of the hourglass modes vanishes, and we obtain

$$(\omega_1^{hour})_{inf.} = (\omega_2^{hour})_{inf.} = \frac{2}{3}\alpha\mu\frac{\Lambda + \alpha\mu/2}{\Lambda + \alpha\mu}\,. \quad (4.4)$$

As it was the original motivation in WILSON et al [1973], the bending response of beam theory is recovered in this case, with the stiffness in bending relying on the axial stiffness of the material. Note that, for $\alpha = 2$ the right-hand-side of (4.4) is proportional to $E/(1-\nu^2)$, the uniaxial stiffness in plane strain infinitesimal elasticity, with E and ν being the standard Young's modulus and Poisson's ratio, respectively, functions of the Lamé constants Λ and μ. We observe also that the hourglass modes become finite in the incompressible limit $\Lambda \to \infty$, thus assuring the characteristic locking-free response of the element, even in finite strain conditions.

Next the case of an Ogden model characterized by $\alpha = 0.5$ is considered. The motivation for this particular choice is to obtain a limit point in the nominal stress/stretch relation. In the incompressible limit, $\lambda_1 = 1/\lambda_2$, we can write

$$P_2 = \frac{\tau_2}{\lambda_2} = \frac{\mu}{\lambda_2}(\lambda_2^\alpha - \lambda_2^{-\alpha})\,, \quad (4.5)$$

for the nominal stress P_2, after using (2.28). Calculation of the tangent modulus for this relation leads to

$$\frac{dP_2}{d\lambda_2} = \frac{\mu}{\lambda_2}\left[(\alpha-1)\lambda_2^\alpha + (\alpha+1)\lambda_2^{-\alpha}\right]\,. \quad (4.6)$$

Setting $dP_2/d\lambda_2 = 0$ results in the critical value of the stretch

$$\lambda_{2,c}^{2\alpha} = \frac{1+\alpha}{1-\alpha}\,. \quad (4.7)$$

a)

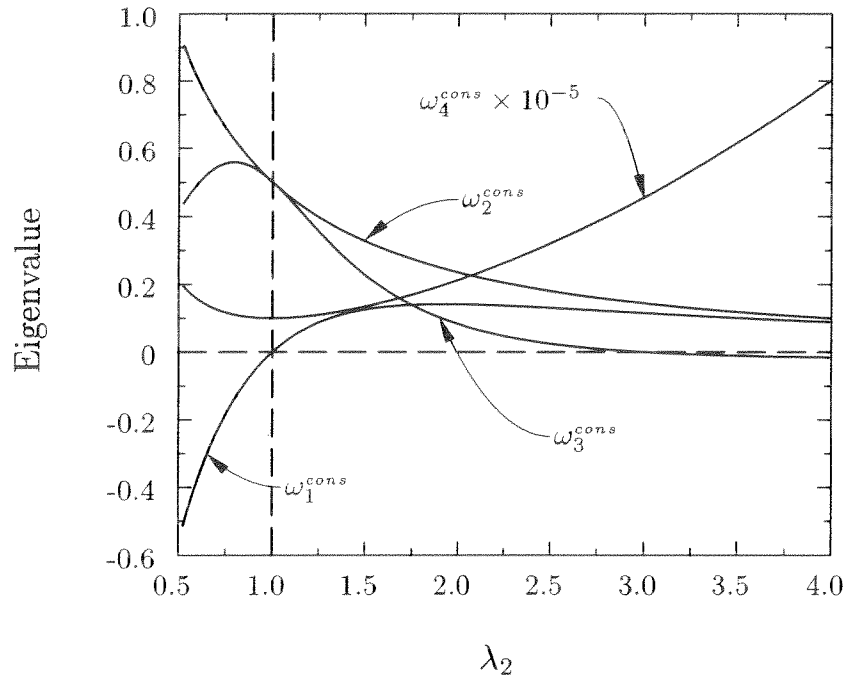

b)

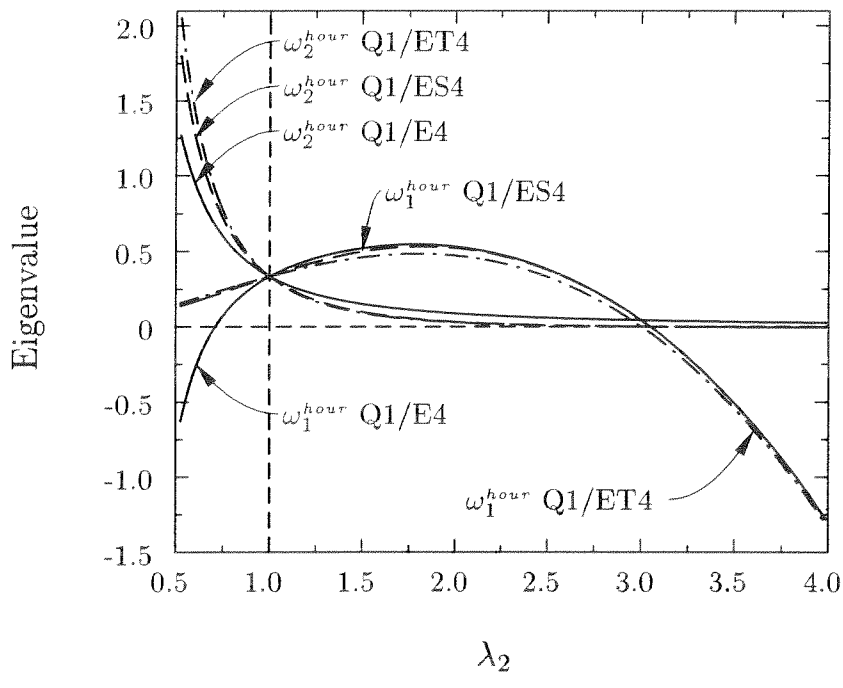

FIGURE 4.1. Ogden model $\alpha = 0.5$, $\Lambda/\mu = 10^5/20$. **a)** Homogeneous deformation modes for all the elements: ω_1^{cons}, infinitesimal rotation; ω_2^{cons}, shearing; ω_3^{cons}, isochoric stretching; and ω_4^{cons}, volumetric (note the scaling). Observe that ω_3^{cons} becomes negative in this physical model. **b)** Hourglass modes for the different elements. Note the negative eigenvalue of the Q1/E4 in compression, and in tension for all the elements just after the stretching eigenvalue ω_3^{cons} becomes negative.

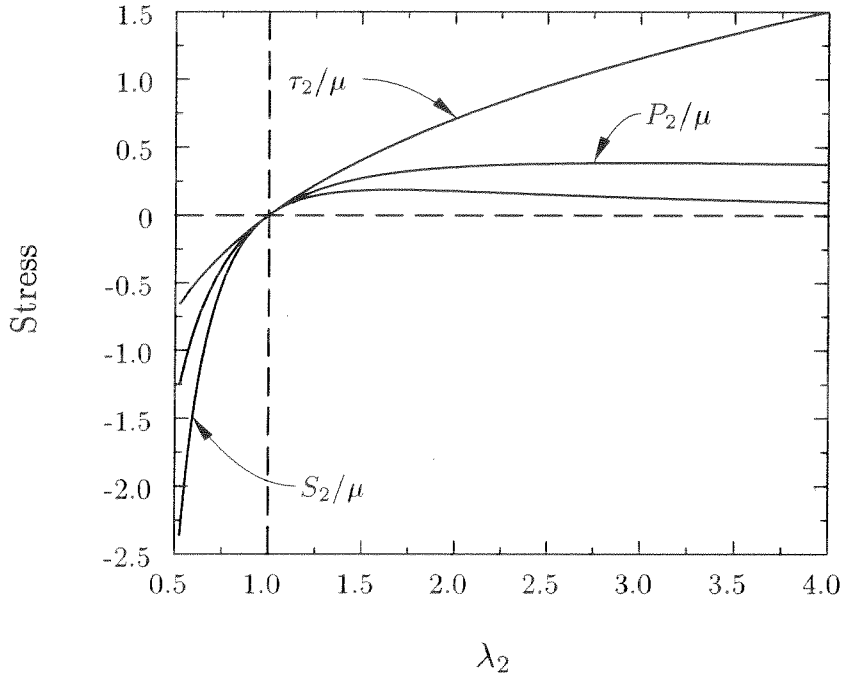

FIGURE 4.2. Ogden model $\alpha = 0.5$, $\Lambda/\mu = 10^5/20$. Axial Kirchhoff stress (τ_2), second Piola-Kirchhoff stress ($S_2 = \tau_2/\lambda_2^2$), and nominal axial stress ($P_2 = \tau_2/\lambda_2$, first Piola-Kirchhoff stress). Observe the limit point in the P_2 (and S_2) law at $\lambda_2 \approx 3$.

The particular choice $\alpha = 0.5$ leads to $\lambda_{2,c} = 3$ in this incompressible limit. Note that no limit point exists for $\alpha > 1$, and that for $0 < \alpha < 1$ the limit point appears in tension only.

We consider again the quasi-incompressible limit characterized by $\Lambda/\mu = 10^5/20$, with $\alpha = 0.5$. Figure 4.2 depicts the nominal stress/stretch relations for this case. We observe the presence of a limit point at $\lambda_{2,c} \approx 3$, with a negative nominal axial stiffness afterwards. This can be observed in the appearance of the negative constant stretching mode ω_3^{cons}. We observe also that the first hourglass mode (bending transversal to the stress direction) becomes negative slightly after the appearance of the physical negative stretching mode in tension. This negative eigenvalue in tension appears in the three elements. The origin of this mode becomes clear after the closed-form expression (3.22) for the hourglass modes, and the discussion above. We observe that the appearance of an axial negative stiffness leads to $\det \boldsymbol{A}^n < 0$, making the stiffness of the hourglass modes negative even if $\det \boldsymbol{A}^s > 0$ in tension. The vanishing of ω_3^{cons} and ω_1^{hour} do not coincide because of the presence of the terms depending on $\boldsymbol{A}^s$ in (3.22). The hourglass modes become negative slightly after the stretching mode.

Further numerical experiments (not shown here) involving general meshes indicate that this mode propagates, leading to a characteristic hourglass pattern in the direction transversal to the load. This situation has been observed in simulations involving finite strain inelastic models, see GLASER & ARMERO [1995], where a similar limit point appears in the stress/stretch relation. In this case, the appearance of this limit point is to be assigned to the plasticity, since Neo-Hookean or Hencky (logarithmic, $\alpha \to \infty$) models are considered for the elastic part. High-order integrations rules reduce the severity of these modes. The reader is referred to this last reference for further details. In compression, the Q1/E4 element still exhibits the zero energy method, whereas the modified $Q1/ES4$ and $Q1/ET4$ elements do not exhibit this drawback.

Remark 4.1. It is to be pointed out again that the motivation behind the consideration of an Ogden model with exponent $\alpha = 0.5$ is the appearance of a limit point in the stress/stretch relation, emulating the observed response in plasticity models. It is known that in order to have an Ogden model satisfying the polyconvexity condition (thus assuring existence of solutions) we must have

$$\alpha\mu > 0 \quad \text{and} \quad |\alpha| \geq 1 \,, \tag{4.8}$$

see OGDEN [1972] and CIARLET [1988]. Given these considerations, the physical significance of the considered model can certainly be argued.

5. Concluding Remarks

A modal analysis of an enhanced finite element in plan strain has been presented for three different enhancement strategies. A general Ogden hyperelastic model has been considered. Results show the appearance of a zero energy method in compression for the original Q1/E4 element. This mode disappears with the modification considered in the Q1/ES4 (based on a full symmetrization of the enhanced field) or the Q1/ET4 quad (based on the transpose of the original enhancement only). Despite these results, it has been shown that zero energy hourglass modes appear in constitutive laws exhibiting limit points (negative axial stiffness). This situation appears to be of particular concern in inelastic simulations.

Acknowledgements: I am indebted to Stefan Glaser and Robert L. Taylor for many helpful discussions.

References

CIARLET, P.G. [1988] *Mathematical Elasticity*, vol. 1, North Holland, Amsterdam.

CRISFIELD, M.A.; G.F. MOITA; G. JELENIC; L.P.R. LYONS & D.R.J. OWEN [1995] 'Enhanced lower-order element formulation for large strains' *Computational Plasticity IV – Fundamentals and Applications – Proceedings of the 4th international conference*, ed. by D.R.J. Owen, E. Onate.

GLASER & ARMERO [1995] "Recent Developments in Enhanced Strain Finite Elements," UCB/SEMM-95/13 Report, December 1995, University of California at Berkeley.

NAGTEGAAL; J.C. & D.D. FOX [1995] "using assumed enhanced strain elements for large compressive deformation," *Int. J. Solid Struct.*, to appear.

OGDEN [1972] "Large Deformation Isotropic Elasticity: on the Correlation of Theory and Experiment for Incompressible Rubberlike Solids," *Proceedings of the Royal Society of London, Series A*, **326,** 565-584.

OGDEN [1984] *"Non-Linear Elastic Deformations,"* John Wiley & Sons, New York.

SIMO, J.C. & S. RIFAI [1990] "A class of mixed assumed strain methods and the method of incompatible modes" *Int. J. Numer. Methods Eng.*, **29**, 1595-1638.

SIMO J.C. & F. ARMERO [1992] "Geometrically non-linear enhanced strain mixed methods and the method of incompatible modes," *Int. J. Numer. Methods Eng.*, **33**, 1413-1449.

SIMO, J.C.; F. ARMERO & R.L. TAYLOR [1993] "Improved versions of assumed enhanced strain tri-linear elements for 3D finite deformation problems," *Comp. Meth. Appl. Mech. Eng.*, **110**, 359-386.

TAYLOR, R.L.; P.J. BERESFORD & E.L. WILSON [1976] "A non-conforming element for stress analysis," *Int. J. Numer. Methods Eng.*, **10**, 1211-1219.

WILSON, E.L., R.L. TAYLOR, W.P. DOHERTY, & J. GHABOUSSI, [1973], "Incompatible displacement models," in *Numerical and Computer Models in Structural Mechanics*, Eds. S.J. Fenves, N. Perrone, A.R. Robinson, and W.C. Schnobrich. Academic Press, New York.

WRIGGERS, P. & S. REESE "A note on enhanced strain methods for large deformations," *Comp. Meth. Appl. Mech. Eng.*, to appear.